






A Simplified Dielectric Material Characterization Algorithm for Both Liquids and Solids

Xiue Bao , *Student Member, IEEE*, Juncheng Bao, *Student Member, IEEE*, Ilja Ocket , *Member, IEEE*,
Song Liu , Dominique Schreurs, *Fellow, IEEE*, Dries Kil , Zhuangzhuang Liu, Meng Zhang,
Robert Puers, *Fellow, IEEE*, and Bart Nauwelaers , *Senior Member, IEEE*

Abstract—A simplified dielectric material characterization technique that combines an equivalent impedance algorithm and a general “line–line” trace method is introduced. The technique is applicable to every type of transmission lines. Due to the convenient fabrication and the allowance of integration with various polymers, coplanar waveguide transmission lines integrated with an SU-8 microfluidic channel is primarily used in this study. The conformal mapping method, an efficient and straightforward way, is introduced to build the foundation of dielectric material characterization and to optimize the sensor design. A validation measurement of the proposed technique is performed on deionized water, and show valuable consistency with previous reliable data presented in the literature. Next, the technique is applied on solid SU-8 characterization with four groups of on-wafer measurements. SU-8 measurement results and the related uncertainty analysis are demonstrated subsequently.

Index Terms—Conformal mapping, coplanar waveguide (CPW), equivalent impedance, microwave measurements, SU-8, trace method.

I. INTRODUCTION

IN THE past decades, dielectric spectroscopy methods have been developed for material characterization [1], [2]. Especially, with the rapid progress in miniaturized technologies, research interests and application requirements on developing low-cost material characterization electronics and instruments have grown exponentially. Representatively, microfluidic

Manuscript received June 1, 2018; revised July 8, 2018; accepted August 14, 2018. This work was supported in part by the Katholieke Universiteit Leuven research project C24/15/015 Microwave Microbiology (μ^2 BIO) and in part by the Hercules project funding. (*Corresponding author: Xiue Bao.*)

X. Bao, J. Bao, D. Schreurs, M. Zhang, and B. Nauwelaers are with the TELEMIC Division of Department of Electrical Engineering (ESAT), Katholieke Universiteit Leuven, Leuven 3001, Belgium (e-mail: xiue.bao@esat.kuleuven.be; juncheng.bao@kuleuven.be; dominique.schreurs@ieec.org; meng.zhang@student.kuleuven.be; Bart.Nauwelaers@esat.kuleuven.be).

I. Ocket is with the TELEMIC Division of Department of Electrical Engineering (ESAT), Katholieke Universiteit Leuven, Leuven 3001, Belgium, and also with the Interuniversity Microelectronics Center, Leuven 3001, Belgium (e-mail: ocket@imec.be).

S. Liu is with Nokia, Hangzhou 310014, China (e-mail: song.liu3000@hotmail.com).

D. Kil and R. Puers are with the Division of ESAT-MICAS, Katholieke Universiteit Leuven, Leuven 3001, Belgium (e-mail: Dries.Kil@esat.kuleuven.be; robert.puers@esat.kuleuven.be).

Z. Liu is with the Material Department, Katholieke Universiteit Leuven, Leuven 3001, Belgium (e-mail: zhuangzhuang.liu@kuleuven.be).

Color versions of one or more of the figures in this paper are available online at <http://ieeexplore.ieee.org>.

Digital Object Identifier 10.1109/TEMC.2018.2866940

structures and polymer-based lab-on-a-chip systems [3], [4], occupying very tiny space but capable of functioning in a complicated way, are playing an increasingly important role. If integrated with passive microwave components, such as coplanar waveguides (CPW), microstrips, capacitors, antennas, resonators, phase shifters, dividers, etc., these structures are suitable for characterizing and detecting various types of solid and liquid materials [1], [5]–[7] with broadband RF, microwave, and even millimeter waves in a real-time label-free measurement approach.

Among the representative applications of the microwave-microfluidic integration, a typical example is using resonators that are based on a variety of structures. Hundreds of studies have been carried out on resonators to improve the sensitivity. Metamaterials, for instance, are even employed in resonator applications for more sensitive measurements [8]. Another increasingly attractive method is calculating the complex permittivity from the propagation constant of transmission lines (e.g., waveguides, coaxial lines, and planar lines). In this determination technique, studying the physical transmission mode [9], [10], extracting the effective permittivity [11], or inferring the distributed per unit length (p.u.l, the unit is “meter”) capacitance and conductance [12], [13] of a transmission line is often involved to extract the permittivity of material under test (MUT).

In terms of the transmission line p.u.l C and G extraction method, two analytical procedures are commonly used. One is directly obtaining C and G from the measured scattering (S -) parameters. Typically, Booth *et al.* [12] and Liu *et al.* [13] determined the p.u.l resistance R , inductance L , capacitance C , and conductance G in different regions of the complete transmission line. Next, after accurately de-embedding the feeding part, they are able to characterize the dielectric MUT perfectly. However, mathematical calculation of feeding parameters and intermediate parameters, such as R and L , makes the procedure complicated and time consuming.

The other approach is utilizing the “line–line” (LL) trace technique [11], [14], [15]. A representative case is characterizing a dielectric material with the calibration comparison method [16]. Two groups of multiline-thru-reflect-line (MTRL) structures are fabricated on a known low-loss substrate and the material to be tested, respectively. With the comparison of the two MTRL calibrations [16], the propagation constant and the characteristic impedance of the transmission lines integrated on the unknown material [17] are accurately obtained. Then, we are able to ar-

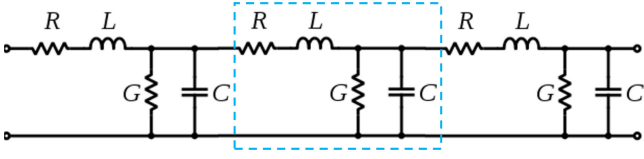


Fig. 1. Equivalent circuit of a CPW transmission line, with a typical section consisting of four distributed frequency-dependent parameters—Capacitance C , conductance G , resistance R , and inductance L .

rive at the p.u.l C and G of the transmission lines fabricated on the unknown material. However, this accurate method is preferable for characterizing solid materials [18] rather than dielectric polymers and liquids. The reason is that the employment of this technique in polymer or liquid measurements might require a complicated device fabrication process.

In this study, we combine an equivalent impedance method [19] with a general LL trace method [14], forming a more straightforward permittivity characterization algorithm. The CPW structure is adopted here, as it is integratable with various microfluidic polymers and easy to fabricate. Additionally, to make the sensor design and permittivity extraction procedure more efficient, the conformal mapping technique [20], [21] is used in the analysis. Deionized (DI) water [22], a representative liquid, is used for validation measurements. Then, SU-8 polymer, first introduced by IBM for electronic applications and then widely used in microfluidic applications because of its excellent lithography properties [23], [24], is measured. The reason is that the rapid development in microwave-microfluidic technology [25] in recent years requires more investigations on the broadband properties of SU-8. Though several techniques have been previously used for SU-8 characterization, they either require a complicated measurement device or need a complicated mathematical process [26].

This paper is organized as follows. Section II first explains the proposed dielectric spectroscopy extraction algorithm based on the combination of an equivalent impedance and a general LL trace technique, and then describes the sensor design principle according to the conformal mapping technique. In Section III, the dielectric material measurement devices and the complete on-wafer measurement setup are introduced. Section IV presents the measurement results and discussions. Conclusions are drawn in Section V.

II. CHARACTERIZATION METHODOLOGY

A. Sensing Theory and Design Approach

We assume that a quasi-TEM mode is propagating through a CPW transmission line, whose electrodes are sandwiched between a h_s thick dielectric substrate ($\epsilon_s, \tan\delta_s$) and a h_m high MUT ($\epsilon_r = \epsilon'_r + j\epsilon''_r$, with $\epsilon''_r = \epsilon'_r \cdot \tan\delta$) [20]. It, thus, can be modeled as an infinite series of two-port elementary sections, as shown in Fig. 1. Each elementary section consists of four frequency-dependent distributed p.u.l parameters— R , L , C , and G . Resistance R and inductance L are independent of the dielectric material on either side of the CPW electrodes, but are only determined by the signal and ground

conductors [12], [27]. According to the conformal mapping technique [20], [21], the distributed p.u.l C and G can be expressed as follows:

$$C = \epsilon_0 \left[2 \frac{K(k_0)}{K(k'_0)} + (\epsilon_s - 1) \frac{K(k_s)}{K(k'_s)} + (\epsilon'_r - 1) \frac{K(k_r)}{K(k'_r)} \right] \quad (1)$$

$$G = \omega \epsilon_0 \left[\epsilon_s \tan\delta_s \frac{K(k_s)}{K(k'_s)} + \epsilon''_r \frac{K(k_r)}{K(k'_r)} \right] \quad (2)$$

where $\epsilon_0 = 8.8542 \cdot 10^{-12}$ F/m is vacuum permittivity; $K(k)$ is the complete elliptic integral of the first kind, and $K(k') = K(\sqrt{1 - k^2})$. The elliptic modulus k_0 and k_i ($i = s, r$) are calculated with the following equations:

$$k_0 = \frac{w}{w + 2s} \sqrt{\frac{1 - (w + 2s)^2 / (w + 2s + 2g)^2}{1 - w^2 / (w + 2s + 2g)^2}} \quad (3)$$

$$k_i = \frac{\sinh(\frac{\pi w}{4h_i})}{\sinh(\frac{\pi(w+2s)}{4h_i})} \sqrt{\frac{1 - \sinh^2(\frac{\pi(w+2s)}{4h_i}) / \sinh^2(\frac{\pi(w+2s+2g)}{4h_i})}{1 - \sinh^2(\frac{\pi w}{4h_i}) / \sinh^2(\frac{\pi(w+2s+2g)}{4h_i})}} \quad (4)$$

where w , g , and s are the signal conductor width, the finite ground width, and the spacing between conductor and ground of the CPW line, respectively.

Therefore, according to expressions (1) and (2), if we adjust the MUT real permittivity ϵ'_r and imaginary permittivity ϵ''_r separately, C and G/ω will linearly change, respectively. Further comparison of (1) and (2) indicates that the coefficients of ϵ'_r and ϵ''_r are with the same values, leading to the following linear relationships [14]:

$$\kappa = \frac{\Delta C}{\Delta \epsilon'_r} = \frac{\Delta G}{\omega \Delta \epsilon''_r} \quad (5)$$

where κ can be easily derived from $\frac{K(k_r)}{K(k'_r)}$, and can also be determined by a two-dimensional (2-D) finite-element simulation method [12]. Therefore, we are able to obtain the dielectric spectroscopy of MUT from the extracted C and G/ω .

Additionally, κ can be also used to determine the optimal size (length and width) and shape of the CPW transmission line sensor. For instance, with given substrate and MUT, if we keep the sum of CPW conductor width and two gaps ($w + 2s$) constant, adjusting the ratio of $w/(w + s)$ and the MUT thickness, we are able to obtain Fig. 2. It is clear that when the MUT height $h_r < (w + 2s)$, capacitance C is very sensitive to h_r , whereas when $h_r \geq (w + 2s)$, capacitance C is almost constant and further increase in MUT thickness does not significantly influence the actual C value. The data obtained under various metallization ratio $w/(w + s)$ values lead to the same conclusion. This means that when the CPW line works as a sensor, the thickness of the to-be-tested material should be larger than $(w + 2s)$ to reduce the measurement uncertainty related to the electromagnetic field distribution. Additionally, with certain MUT, a larger $w/(w + s)$ ratio is associated with a larger capacitance C , which indicates higher measurement sensitivity for the complex permittivity extraction.

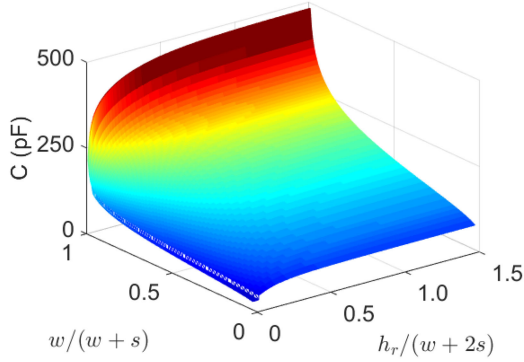


Fig. 2. Variation of calculated C due to different metal-gap ratio $w/(w+s)$ and MUT height, with constant $(w+2s)$.

B. Characterization Mechanism

Assume that there are two identical CPW transmission lines fabricated on a low-loss substrate. One line is loaded with a reference material of known permittivity, and the other line is covered with the dielectric MUT. The length of the reference material line is l_r , and its propagation constant, p.u.l capacitance, and p.u.l conductance are denoted as γ_r , C_r , and G_r , respectively. The corresponding parameters of the test line are l_t , γ_t , C_t , and G_t , respectively. Measured S -parameters of the two lines are transformed into cascade matrices M_r and M_t by [28]

$$M_i = \frac{1}{S_{21i}} \begin{bmatrix} (S_{12i}S_{21i} - S_{11i}S_{22i}) & S_{11i} \\ -S_{22i} & 1 \end{bmatrix} \quad (6)$$

where S -parameters S_i of the reference/test CPW line can be calibrated [11], [13] or uncalibrated [29], but are recommended to be switch-term corrected [30]. For a dielectric MUT, the distributed R and L of the test line are the same as the identical reference line, because R and L are only determined by the electrodes' geometries and properties. The two lines have the following relationship [14]:

$$\begin{aligned} \text{Tr}[M_t \cdot M_r^{-1}] &= 2 \cosh(\gamma_r \cdot l_r) \cdot \cosh(\gamma_t \cdot l_t) \\ &\quad - \left(\frac{\gamma_r}{\gamma_t} + \frac{\gamma_t}{\gamma_r} \right) \cdot \sinh(\gamma_r \cdot l_r) \cdot \sinh(\gamma_t \cdot l_t), \end{aligned} \quad (7)$$

where $\text{Tr}[X]$ denotes the trace operation of matrix X .

According to the equivalent impedance theory [19], we are able to arrive at an expression that directly relates the unknown C_t and G_t to the known parameters as follows [28]:

$$\frac{\gamma_t}{\gamma_r} = \sqrt{\frac{G_t + j\omega C_t}{G_r + j\omega C_r}}. \quad (8)$$

If we utilize a bare line as the reference transmission line (i.e., air works as the reference material), its distributed conductance G_r is negligible when the employed substrate has low-loss property. Its distributed capacitance C_r is readily obtained from (1) or by a 2-D simulation of the CPW line cross section [12]. We can

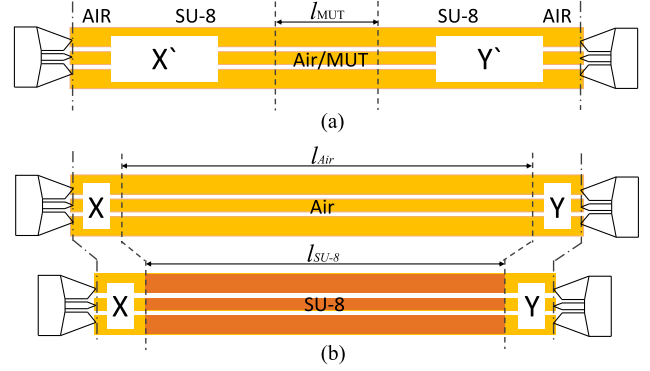


Fig. 3. Schematics of a microfluidic line, a bare line, and a SU-8 line. (a) Liquid permittivity characterization. (b) Dielectric SU-8 characterization, where X, Y, X', and Y' are the de-embedding error boxes.

also arrive at the accurate C_r with the resistance measurement technique [31].

With known C_r and G_r , we can use (5) to estimate C_t and G_t by reasonably estimating the permittivity of the tested material. With the estimated C_t and G_t , we can subsequently arrive at the estimated γ_t according to the relationship in (8). Next, the estimated γ_t is put into the right part of formula (7), and therefore, an estimated $\text{Tr}[M_2 \cdot M_1^{-1}]^{\text{est}}$ is calculated. By fitting the estimated $\text{Tr}[M_2 \cdot M_1^{-1}]^{\text{est}}$ to the actually measured $\text{Tr}[M_2 \cdot M_1^{-1}]$ with a least-squares optimization algorithm, the final C_t and G_t are obtained. Subsequently, the complex relative permittivity of the tested dielectric material can be inferred from C_t and G_t according to (5).

III. DEVICES DESIGN AND FABRICATION

A. Coplanar Sensor Design

The measurement devices are schematically shown in Fig. 3, where l_{MUT} , l_{AIR} , and $l_{\text{SU-8}}$ represent the sensing area. Generally, there are three types of CPW lines used in this study. For liquid characterization, an SU-8 microfluidic structure is designed on top of the CPW line to confine liquids onto the CPW sensing region, as shown in Fig. 3(a). This complete device can be divided into five regions, including one sensing region, two bare line feeding regions, and two SU-8 loaded feeding regions. The two bare feeding regions are designed with the same dimension, and also the two SU-8 feeding regions have the same structure and dimensions. Regarding the solid material measurement, taking SU-8 polymer characterization as an example in this study, a bare line and another line loaded with SU-8 are required, both of which have arbitrary lengths [shown in Fig. 3(b)].

B. Microwave Device Fabrication

The devices are fabricated on a 4-in Borofloat 33 glass ($\epsilon_r = 4.6$, $\tan \delta = 0.0037$ at 10 MHz and 25 °C) wafer. Fig. 4(a) summarizes the standard lift-off fabrication procedure of the CPW electrodes [32]. Prior to the lithography process, the glass wafer is cleaned in a boiling Piranha solution ($\text{H}_2\text{SO}_4:\text{H}_2\text{O}_2 = 3:1$) for 10 min. It is followed by a dehydration process

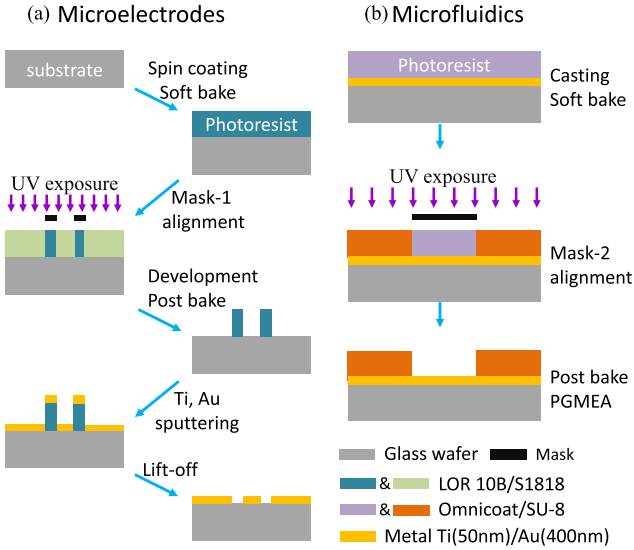


Fig. 4. Schematic diagrams. (a) CPW electrodes fabrication sequence. (b) SU-8 microfluidic layer patterning procedure.

under 200 °C for 2 min. Next, LOR 10B and S1818 photoresists are spin coated on the glass wafer separately, each with a thickness of 1 μm . After soft baking, the two photoresist layers are exposed to UV light through a pattern mask, and then they are developed in the related photoresist developer (351 Dev:H₂O=1:4) to remove the exposed part. Subsequently, a 50-nm-thick Ti adhesion layer followed by a 400-nm-thick Au layer is deposited using sputter deposition. The final lift-off process for electrodes fabrication is completed by immersing the glass wafer in N-Methylpyrrolidone for two days to remove the rest LOR 10B and S1818 photoresists together with the unwanted metal parts.

The fabricated electrodes form the CPW sensing structures and the MTRL calibration standards [33]. The signal width w , ground width g , and spacing s at the cross section of these CPW lines are 20 μm , 100 μm , and 150 μm , respectively. The lengths of the CPW transmission lines used as MTRL calibration standards are 0.42 mm (thru), 0.21 mm (short), 1 mm, 2.155 mm, 5.933 mm, 11.5 mm, 20.53 mm, respectively.

After obtaining the wafer with patterned Ti/Au electrodes, a 350- μm SU-8 polymer layer is defined with the technique depicted in Fig. 4(b). About 1- μm layer of MicroChem OmniCoat is first spin coated on the glass wafer and soft baked on a hot plate for 1 min at 200 °C. Then, 6 g of SU-8 2005 is poured and evenly spread on the glass wafer that has been put on a flat plate. The SU-8 2005 (45% solids) is prepared by dissolving SU-8 2050 (71.65% solids) into the organic solvent SU-8 2000 thinner (MicroChem Corporation). The soft-baking process is performed on a hotplate for 24 h at 80 °C, in order to partially evaporate the solvent content before exposure [34]. After soft baking, solid concentration of the casted SU-8 is around 93%. The patterning of the SU-8 film is done by exposing to near-UV light through a mask. After exposure to near-UV light and postbaking procedure, it is developed in a propylene-glycol-methyl-ether-acetate developer (MicroChem Corporation) for 80 s and rinsed with acetone and DI water, leaving only the

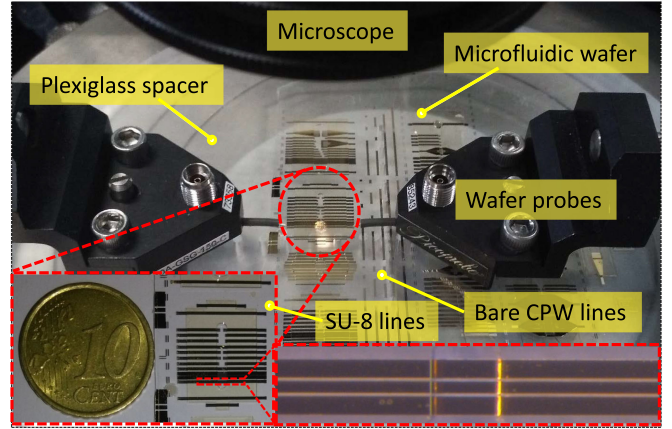


Fig. 5. On-wafer measurement setup for dielectric material characterization, with a zoomed in view highlighting the microfluidic device.

cross-linked SU-8 pattern. Hard backing is avoided after the developing process so as to assure the SU-8 tightly sticking to the glass wafer.

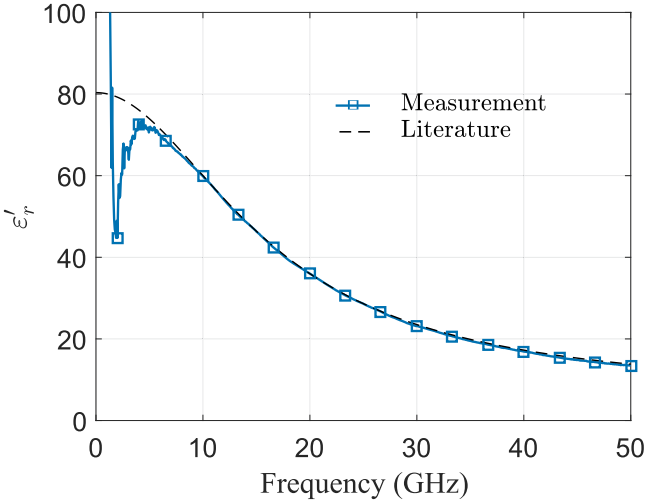
IV. MEASUREMENT RESULTS AND DISCUSSION

A. Measurement Setup

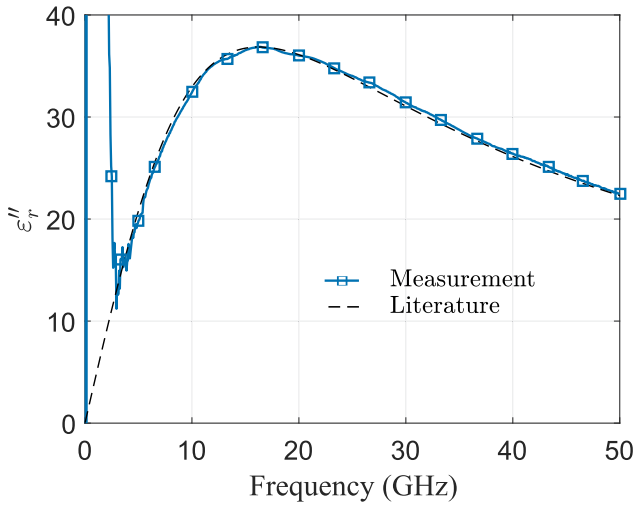
The complete measurement setup is depicted in Fig. 5. The on-wafer measurements were performed on a Cascade Microtech probe station equipped with a thermal chuck. Two 40A-GSG-150C ground-signal-ground microwave Picoprobes (GGB Industries) connected to an Agilent E8361A vector network analyzer (VNA) were utilized. The measurement frequency was swept from 10 MHz to 50 GHz, and the VNA power was set at -20 dBm to reduce any microwave heating effects. During the measurements, an 8-mm-thick plexiglass ($\epsilon_r = 2.593$, $\tan \delta = 0.022$ around 10 GHz [35]) spacer was placed under the device to reduce the parasitic microstrip mode between the CPW conductors and the metal chuck. During liquid measurement, the lab temperature was kept at 20 °C and a digital thermocouple was used to monitor the real-time temperature. All measured S -parameters will be first calibrated with the MTRL calibration technique using the CPW standards that are described in the previous section.

B. Liquid Water Characterization

The dielectric spectroscopy of DI water has been illustrated in the literature in detail with bulk measurement techniques [22]. It is thus used here to validate the characterization mechanism proposed in previous sections. The validation procedure was performed on the symmetrical CPW line integrated with a microfluidic channel, as shown in Fig. 3(a) and the inset photos of Fig. 5. The channel length at the sensing area is 1.5 mm, and the lengths of the two bare feeding lines and the two SU-8 feeding lines are 1.5 mm and 4.5 mm, respectively. In order to use the empty device as the reference, the S -parameters were recorded before and after loading DI water. During this process, the probes were kept stable to avoid any error caused by the



(a)



(b)

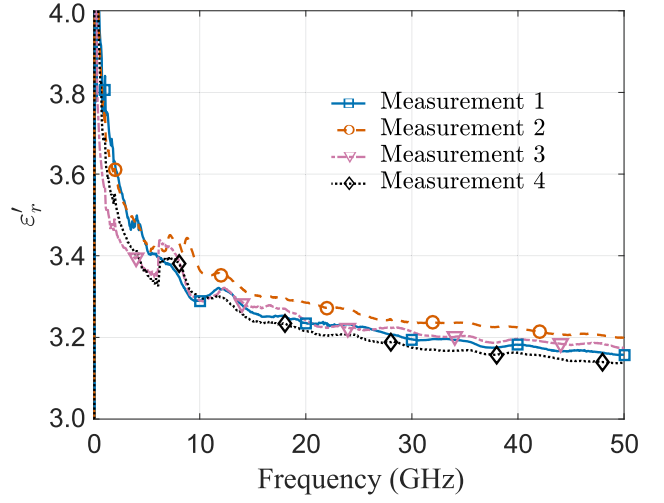
Fig. 6. Measured dielectric spectroscopy of DI water at 19.6 °C together with values reported in [22].

connection difference. The measured liquid temperature was 19.6 °C.

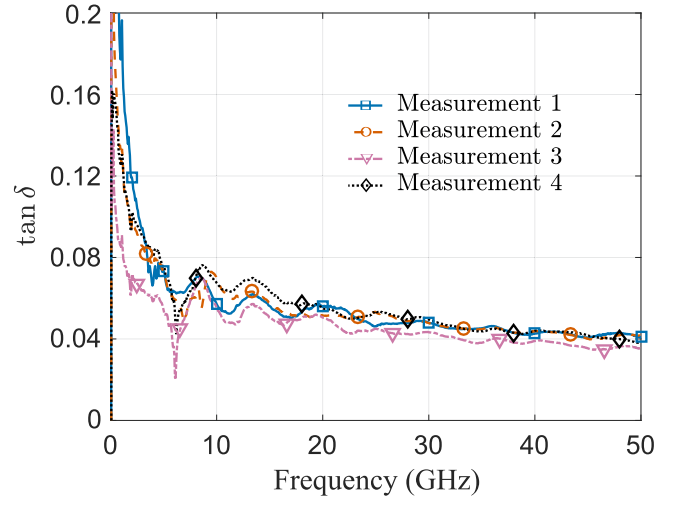
Combination of (7), (8), (1), and (5) leads to the complex permittivity measurement results of DI water. As shown in Fig. 6, the acquired complex permittivity shows good consistency with literature values [22] at high frequencies. The average relative error of the water permittivity measurement from 5 to 50 GHz is 1.382%. The obvious deviation at low frequencies (lower than 5 GHz in this study) is mainly related to the length of the sensing region, and can dramatically decrease if a much longer sensing line is applied [13]. Regardless of this, the results have revealed the feasibility of the proposed method for characterizing dielectric materials at frequencies higher than about 5 GHz.

C. Solid SU-8 Characterization

Four groups of measurements were performed for SU-8 characterization using the sensing structures schematically, as shown in Fig. 3(b). Measurements named “Measurement 1” and “Measurement 2” were performed with a 10.5-mm-long SU-8 line and



(a)



(b)

Fig. 7. Measured dielectric spectroscopy of solid SU-8 at 19.6 °C. A 10.5-mm-long SU-8 line is utilized to compare with a 8.5-mm bare line, a 2.933-mm-long bare line, a 4.4-mm-long SU-8 line, and a 2-mm-long SU-8 line for “Measurement 1,” “Measurement 2,” “Measurement 3,” and “Measurement 4,” respectively.

two different bare lines of lengths 8.5 mm and 2.933 mm, respectively. Measurements named “Measurement 3” and “Measurement 4” still used the 10.5-mm SU-8 line yet comparing with two other SU-8 CPW lines of different lengths. The lengths of the other two SU-8 lines are 2 mm and 4.4 mm, respectively. The measured temperature was 19.6 °C.

The measurement results of the SU-8 relative dielectric constant ϵ_r and loss tangent $\tan \delta$ are shown in Fig. 7. Ignoring the values at low frequencies (i.e., lower than about 5 GHz, within which there is higher measurement uncertainty), we observe frequency-dependent properties in ϵ_r and $\tan \delta$. Specifically, when the frequency increases from around 5 to 50 GHz, SU-8 ϵ_r decreases from about 3.4 to about 3.2, and its $\tan \delta$ drops from around 0.07 to 0.04. The measurement results are slightly different from literature values [26], [36], [37]. For example, Mbairi and Hesselbom [26] used conductor-backed CPW lines and obtained an averaged relative dielectric constant value of

3.25 and a loss tangent value of 0.027 at 30 GHz, whereas, in [36], a relative dielectric constant of 2.85 and a loss tangent of 0.04 at 25 GHz were determined based on microstrip lines. These obvious differences might partly relate to the difference in fabrication procedure and the utilized chemical materials in SU-8 preparation.

Furthermore, obvious deviations are also observed in the results obtained from the four different approaches. One possible error source might be the difference in probe placement for the different lines. Another cause that should not be ignored might also be the fabrication tolerance. To the authors' investigations, neither the Ti/Au electrode layer nor the SU-8 layer is uniform enough, which might also lead to a difference in the error boxes X and Y, resulting in a permittivity extraction error. Moreover, there is some fabrication error for each device due to any time difference or chemical difference, which might also result in some errors in the measurements. For instance, the dielectric properties of the SU-8 layer are very sensitive to the lift-off fabrication conditions [34], [38].

Theoretically, MTRL calibration has negligible effects on the permittivity extraction procedure because the LL trace method only focuses on the difference between the two transmission lines [14]. Therefore, the SU-8 characterization error mainly comes from the two CPW lines used in each measurement group. Uncertainty analysis based on perturbation was performed to study the effects of probe placement and device fabrication error. 5 μm of the probe placement error and 0.5 μm of the length fabrication error were considered in the two CPW lines. The probe placement error can be at either the left or the right port of the reference line, or at either the left or the right port of the tested SU-8 line, resulting in four possibilities. For each possibility, the probe placement results in an error in the cascade matrices either M_r or M_t , and therefore, leads to an error in the measured MUT permittivity result. The total uncertainty due to 5- μm probe placement error is calculated with the following formulas:

$$u(\varepsilon'_r) = \sqrt{\sum_{n=1}^4 (\varepsilon'_{rn} - \varepsilon'_{r0})^2} \quad (9)$$

$$u(\tan \delta) = \sqrt{\sum_{n=1}^4 (\tan \delta_n - \tan \delta_0)^2} \quad (10)$$

where ε'_{r0} and $\tan \delta_0$ denote the measured SU-8 dielectric constant and loss tangent, respectively, when there is not any probe placement error. Similarly, the 0.5- μm length fabrication error can happen on either the reference bare line or the tested SU-8 line, resulting in two possibilities. Using the same calculation procedure as the fabrication error, the uncertainty due to the fabrication tolerance can be arrived at.

The uncertainties on the SU-8 dielectric constant and loss tangent measurements are shown in Fig. 8. It is clear that compared to the probe placement error, the uncertainties due to fabrication tolerance in length are ignorable. Furthermore, the combination of two SU-8 lines (i.e., "Measurement 3" and "Measurement 4") seems to show lower and more stable uncertainties than the combination of an SU-8 line with a bare line (i.e., "Measurement 1" and "Measurement 2"). Besides, the

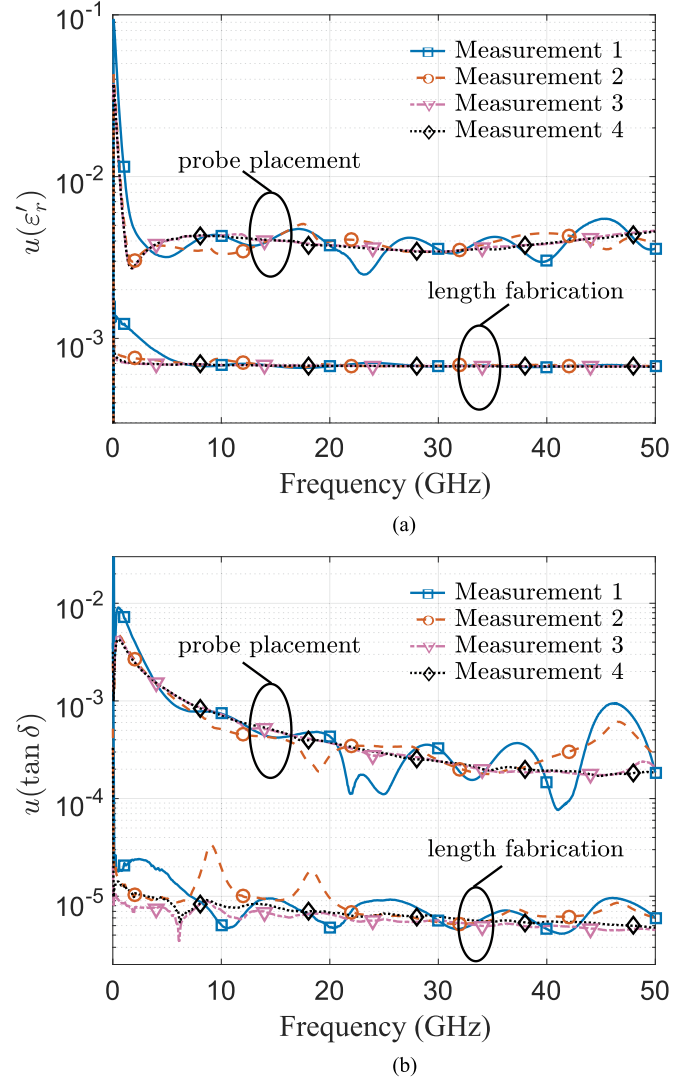


Fig. 8. Uncertainties of SU-8 dielectric parameters due to 5- μm probe placement difference and 0.5- μm fabrication length error.

lower uncertainties $u(\tan \delta)$ of the two SU-8 line approach at higher frequencies have preliminarily validated the advantage of the proposed method in material characterization within high frequency range.

V. CONCLUSION

An algorithm that combines the equivalent impedance method with a general LL trace method is developed for dielectric material characterization. The technique requires less intermediate variables calculation procedure. In addition, introduction of conformal mapping method in the sensor design makes the method more efficient and money saving. Validation measurements on DI water have shown the feasibility of using this technique to extract accurate permittivities at high frequencies. Next, the method is used for characterizing SU-8 polymer with four groups of CPW lines. Uncertainty studies show that the two SU-8 line approach results in better measurement results.

ACKNOWLEDGMENT

The authors would like to express their gratitude to Katholieke Universiteit Leuven NanoCenter for their valuable technical input and assistance to FabLab for plexiglass spacer fabrication, and to colleagues in TELEMIC for productive discussions.

REFERENCES

- [1] A. Hosseinbeig, S. Marathe, and D. Pommerenke, "Characterization of relative complex permittivity and permeability for magneto-dielectric sheets," *IEEE Trans. Electromagn. Compat.*, vol. 60, no. 6, pp. 1786–1794, Dec. 2018.
- [2] J. Zhang *et al.*, "Reconstruction of dispersive dielectric properties for PCB substrates using a genetic algorithm," *IEEE Trans. Electromagn. Compat.*, vol. 50, no. 3, pp. 704–714, Aug. 2008.
- [3] P. Yager *et al.*, "Microfluidic diagnostic technologies for global public health," *Nature*, vol. 442, no. 7101, pp. 412–418, 2006.
- [4] H. Becker and C. Gärtner, "Polymer microfabrication methods for microfluidic analytical applications," *Electrophoresis*, vol. 21, no. 1, pp. 12–26, 2000.
- [5] A. Bababjanyan, H. Melikyan, S. Kim, J. Kim, K. Lee, and B. Friedman, "Real-time noninvasive measurement of glucose concentration using a microwave biosensor," *J. Sensors*, vol. 2010, 2010, Art. no. 452163.
- [6] J. Do and C. H. Ahn, "A polymer lab-on-a-chip for magnetic immunoassay with on-chip sampling and detection capabilities," *Lab Chip*, vol. 8, no. 4, pp. 542–549, 2008.
- [7] U. C. Hasar and Y. Kaya, "Self-calibrating noniterative complex permittivity extraction of thin dielectric samples," *IEEE Trans. Electromagn. Compat.*, vol. 60, no. 2, pp. 354–361, Apr. 2018.
- [8] A. Ebrahimi, W. Withayachumnankul, S. Al-Sarawi, and D. Abbott, "High-sensitivity metamaterial-inspired sensor for microfluidic dielectric characterization," *IEEE Sensors J.*, vol. 14, no. 5, pp. 1345–1351, May 2014.
- [9] M. Janezic and J. A. Jargon, "Complex permittivity determination from propagation constant measurements," *IEEE Microw. Guided Wave Lett.*, vol. 9, no. 2, pp. 76–78, Feb. 1999.
- [10] D. F. Williams and C. L. Holloway, "Transmission-line parameter approximation for digital simulation," *IEEE Trans. Electromagn. Compat.*, vol. 43, no. 4, pp. 466–470, Nov. 2001.
- [11] K. Grenier *et al.*, "Integrated broadband microwave and microfluidic sensor dedicated to bioengineering," *IEEE Trans. Microw. Theory Techn.*, vol. 57, no. 12, pp. 3246–3253, Dec. 2009.
- [12] J. C. Booth, N. D. Orloff, J. Mateu, M. Janezic, M. Rinehart, and J. A. Beall, "Quantitative permittivity measurements of nanoliter liquid volumes in microfluidic channels to 40 GHz," *IEEE Trans. Instrum. Meas.*, vol. 59, no. 12, pp. 3279–3288, Dec. 2010.
- [13] S. Liu *et al.*, "Hybrid characterization of nanoliter dielectric fluids in a single microfluidic channel up to 110 GHz," *IEEE Trans. Microw. Theory Techn.*, vol. 65, no. 12, pp. 5063–5073, Dec. 2017.
- [14] X. Bao *et al.*, "A general line–line method for dielectric material characterization using conductors with the same cross-sectional geometry," *IEEE Microw. Wireless Compon. Lett.*, vol. 28, no. 4, pp. 356–358, Apr. 2018.
- [15] N. J. Farcich, J. Salonen, and P. M. Asbeck, "Single-length method used to determine the dielectric constant of polydimethylsiloxane," *IEEE Trans. Microw. Theory Techn.*, vol. 56, no. 12, pp. 2963–2971, Dec. 2008.
- [16] D. F. Williams, R. B. Marks, and A. Davidson, "Comparison of on-wafer calibrations," in *Proc. 38th ARFTG Conf.*, San Diego, CA, USA, 1991, pp. 68–81.
- [17] D. F. Williams and R. B. Marks, "Accurate transmission line characterization," *IEEE Microw. Guided Wave Lett.*, vol. 3, no. 8, pp. 247–249, Aug. 1993.
- [18] N. Orloff, J. Mateu, M. Murakami, I. Takeuchi, and J. C. Booth, "Broadband characterization of multilayer dielectric thin-films," in *Proc. IEEE MTT-S Int. Microw. Symp.*, Honolulu, HI, USA, 2007, pp. 1177–1180.
- [19] M. D. Janezic and D. F. Williams, "Permittivity characterization from transmission-line measurement," in *Proc. IEEE MTT-S Int. Microw. Symp.*, 1997, pp. 1343–1346.
- [20] W. Heinrich, "Quasi-TEM description of MMIC coplanar lines including conductor-loss effects," *IEEE Trans. Microw. Theory Techn.*, vol. 41, no. 1, pp. 45–52, Jan. 1993.
- [21] G. Ghione and C. U. Naldi, "Coplanar waveguides for MMIC applications: Effect of upper shielding, conductor backing, finite-extent ground planes, and line-to-line coupling," *IEEE Trans. Microw. Theory Techn.*, vol. MTT-35, no. 3, pp. 260–267, Mar. 1987.
- [22] W. J. Ellison, "Permittivity of pure water, at standard atmospheric pressure, over the frequency range 0–25 THz and the temperature range 0–100 °C," *J. Phys. Chem. Ref. Data*, vol. 36, no. 1, pp. 1–18, Mar. 2007.
- [23] H. Lorenz, M. Despont, N. Fahrni, N. LaBianca, P. Renaud, and P. Vettiger, "SU-8: A low-cost negative resist for MEMS," *J. Micromech. Microeng.*, vol. 7, no. 3, pp. 121–124, 1997.
- [24] K. Lee *et al.*, "Micromachining applications of a high resolution ultrathick photoresist," *J. Vac. Sci. Technol. B, Microelectron. Nanometer Struct. Process. Meas. Phenom.*, vol. 13, no. 6, pp. 3012–3016, 1995.
- [25] X. Bao, I. Ocket, D. Kil, J. Bao, R. Puers, and B. Nauwelaers, "Liquid measurements at microliter volumes using 1-port coplanar interdigital capacitor," in *Proc. IEEE MTT-S Microw. Bio Conf.*, Gothenburg, Sweden, 2017, pp. 1–4.
- [26] F. D. Mbairi and H. Hesselbom, "High frequency design and characterization of SU-8 based conductor backed coplanar waveguide transmission lines," in *Proc. Int. Symp. Adv. Packag. Mater. Processes, Properties, Interfaces*, Irvine, CA, USA, 2005, pp. 243–248.
- [27] A. Scarlatti and C. L. Holloway, "An equivalent transmission-line model containing dispersion for high-speed digital lines-with an FDTD implementation," *IEEE Trans. Electromagn. Compat.*, vol. 43, no. 4, pp. 504–514, Nov. 2001.
- [28] R. B. Marks and D. F. Williams, "A general waveguide circuit theory," *J. Res. Nat. Inst. Standards Technol.*, vol. 97, no. 5, pp. 533–562, Sep./Oct. 1992.
- [29] Z. Caijun, J. Quanxing, and J. Shenhui, "Calibration-independent and position-insensitive transmission/reflection method for permittivity measurement with one sample in coaxial line," *IEEE Trans. Electromagn. Compat.*, vol. 53, no. 3, pp. 684–689, Aug. 2011.
- [30] R. B. Marks, "Formulations of the basic vector network analyzer error model including switch-terms," in *Proc. 50th ARFTG Conf.* Portland, OR, USA, 1997, pp. 115–126.
- [31] D. F. Williams and R. B. Marks, "Transmission line capacitance measurement," *IEEE Microw. Guided Wave Lett.*, vol. 1, no. 9, pp. 243–245, Sep. 1991.
- [32] S. D. Minter, *Microfluidic Techniques Reviews and Protocols*. New York, NY, USA: Humana Press, 2006.
- [33] R. B. Marks, "A multilayer method of network analyzer calibration," *IEEE Trans. Microw. Theory Techn.*, vol. 39, no. 7, pp. 1205–1215, Jul. 1991.
- [34] T. A. Anhoj, A. M. Jorgensen, D. A. Zauner, and J. Hübner, "The effect of soft bake temperature on the polymerization of SU-8 photoresist," *J. Micromech. Microeng.*, vol. 16, no. 9, pp. 1819–1824, 2006.
- [35] U. C. Hasar and C. R. Westgate, "A broadband and stable method for unique complex permittivity determination of low-loss materials," *IEEE Trans. Microw. Theory Techn.*, vol. 57, no. 2, pp. 471–477, Feb. 2009.
- [36] A. Ghannam, C. Viallon, D. Bourrier, and T. Parra, "Dielectric microwave characterization of the SU-8 thick resin used in an above IC process," in *Proc. Eur. Microw. Conf.*, Rome, Italy, 2009, pp. 1041–1044.
- [37] J. M. Dewdney and J. Wang, "Characterization of the microwave properties of SU-8 based on microstrip ring resonator," in *Proc. Wireless Microw. Technol. Conf.*, Clearwater, FL, USA, 2009, pp. 1–5.
- [38] R. Feng and R. J. Farris, "Influence of processing conditions on the thermal and mechanical properties of SU8 negative photoresist coatings," *J. Micromech. Microeng.*, vol. 13, no. 1, pp. 80–88, 2002.



Xiue Bao (S'17) was born in Baoding, China. She received the B.Sc. degree in information engineering and the M.Sc. degree in metallurgical engineering from the University of Science and Technology Beijing, Beijing, China, in 2011 and 2013, respectively. She is currently working toward the Ph.D. degree in electrical engineering at the University of Leuven, Leuven, Belgium.

Her research interests focus on microwave biomedical applications, including broadband dielectric spectroscopy, biosensor design, microwave-microfluidic structure design and fabrication, RF, microwave, and millimeter-wave measurement and calibration.

Ms. Bao was the recipient of the IEEE Microwave Theory and Techniques Society Graduate Fellowship in 2018.



Juncheng Bao (S'17) received the M.Sc. degree in electrical engineering in 2013 from Katholieke Universiteit Leuven, Leuven, Belgium, where he is currently working toward the Ph.D. degree in electrical engineering.

He had an internship with imec, Leuven, in 2013. His research interests include microwave biomedical applications, novel microwave-microfluidic devices design and fabrication, and microwave and millimeter-wave metrology.



Dries Kil received the M.S. degree in nanoscience and nanotechnology from the Katholieke Universiteit Leuven, Leuven, Belgium, in 2014. The subject of the M.S. thesis was the design and fabrication of a novel neurotrophic electrode based on controlled growth factor release. Since October 2014, he has been working toward the Ph.D. degree in electrical engineering at the MICAS group, Katholieke Universiteit Leuven.

Since October 2014, he has also been a Research Assistant with the MICAS group, under the guidance of Prof. R. Puers. His research interest includes the development of flexible neural probes with a strong focus on biocompatibility and tissue integration.

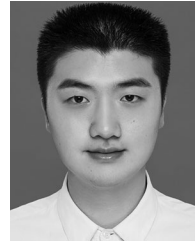


Ilja Ocket (M'09) received the M.Sc. and Ph.D. degrees in electrical engineering from Katholieke Universiteit Leuven (KU Leuven), Leuven, Belgium, in 1998 and 2009, respectively.

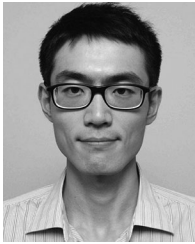
Since 1999, he has been with imec, Leuven, Belgium, and with KU Leuven. With imec, he is currently involved in millimeter-wave antenna modules and packaging for 79- and 140-GHz radar. With KU Leuven, he leads the group working in the area of microwave and millimeter-wave applications for biology and medicine, and is also involved in integrated

couplers for (sub)millimeter plastic waveguides.

Zhuangzhuang Liu's, photograph and biography not available at the time of publication.



Meng Zhang received the B.S. degree in electrical engineering from the University of Electronic Science and Technology of China, Chengdu, China, in 2013, and the M.S. degree in electrical engineering from the University of Leuven, Leuven, Belgium, in 2016. Since 2017, he has been following the Postgraduate Program of Biomedical Engineering with the University of Leuven, where he is currently working toward the Ph.D. degree with a focus on highly sensitive broadband dielectric spectroscopy for biomedical applications.



Song Liu received the Ph.D. degree in electrical engineering from Katholieke Universiteit Leuven (KU Leuven), Leuven, Belgium, in 2016.

In 2014 and 2015, he spent six months with the RF Technology Division, National Institute of Standards and Technology, Boulder, CO, USA, under the support of KU Leuven. His research interests include RF power amplifier design, microwave biomedical applications, vector network analyzer calibration, and material characterization.

Dr. Liu was the recipient of the Automatic RF Techniques Group Roger Pollard Student Fellowship in 2013 and the IEEE Microwave Theory and Techniques Society Graduate Fellowship in 2014.



Robert Puers (M'86–SM'95–F'11) received the Ph.D. degree from Katholieke Universiteit Leuven (KU Leuven), Leuven, Belgium, in 1986.

At KU Leuven, he became the Director of the Clean Room Facilities for Silicon and Hybrid Circuit Technology with the ESAT-MICAS laboratories. He was a European pioneer in the research on micromachining, MEMS, and packaging techniques, mainly for biomedical implantable systems. To this purpose, he assembled the requested infrastructure, and installed a clean room in 1984, which now runs for

more than 25 years under his guidance. Recently, microfluidic and optical MEMS based on polymers are forming the backbone of his sensor research. Besides MEMS, his work focuses also on low-power systems, smart interfaces, inductive power, and wireless communication. He authored/coauthored design guidelines to improve the efficiency of power induction in two books. He took major efforts to increase the impact of MEMS and microsystems in both the international research community as well as in industry. He helped to launch two spin-off companies.



Dominique Schreurs (S'90–M'97–SM'02–F'12) received the M.Sc. degree in electronic engineering and the Ph.D. degree from the University of Leuven (KU Leuven), Leuven, Belgium in 1992 and 1997, respectively.

She is currently a Full Professor and a Chair of LICT with KU Leuven, Leuven, Belgium. She has been a Visiting Scientist with Agilent Technologies, Santa Rosa, CA, USA; ETH Zurich, Zurich, Switzerland; and the National Institute of Standards and Technology, Boulder, CO, USA. Her research

interests include the microwave and millimeter-wave characterization and modeling of active devices and bioliquids, as well as the system design for wireless communications and biomedical applications.

Dr. Schreurs is the IEEE MTT-S President, a former MTT-S Distinguished Microwave Lecturer, and an Editor-in-Chief for the IEEE TRANSACTIONS ON MICROWAVE THEORY AND TECHNIQUES. She is also a President of the ARFTG organization, and was a General Chair of the 2007, 2012, and 2018 ARFTG conferences.



Bart Nauwelaers (S'80–M'86–SM'99) received the master's degree in design of telecommunication systems from Telecom ParisTech, Paris, France, in 1981 and the Ph.D. degree in electrical engineering from the Katholieke Universiteit (KU Leuven), Leuven, Belgium, in 1988.

Since 1981, he has been with the Department of Electrical Engineering, KU Leuven, where he has been involved in research on microwave antennas, passive components, interconnects, microwave integrated circuits and MMICs, linear and nonlinear device modeling, MEMS, and wireless communications.

Dr. Nauwelaers is the former Chair of the IEEE AP/MTT-Benelux and the past Chair of URSI-Benelux.